analytical chemistry

Article

pubs.acs.org/ac

# Simultaneous Analysis of Major Coenzymes of Cellular Redox Reactions and Energy Using ex Vivo $^1$H NMR Spectroscopy

G. A. Nagana Gowda,*[,†,‡] Lauren Abell,[‡] Chi Fung Lee,[‡] Rong Tian,[‡] and Daniel Raftery*[,†,‡,§,∥]

[†]Northwest Metabolomics Research Center, [‡]Mitochondria and Metabolism Center, Anesthesiology and Pain Medicine, and [§]Department of Chemistry, University of Washington, Seattle, Washington 98109, United States

[∥]Fred Hutchinson Cancer Research Center, Seattle, Washington 98109, United States

Supporting Information

**ABSTRACT:** Coenzymes of cellular redox reactions and cellular energy mediate biochemical reactions fundamental to the functioning of all living cells. Despite their immense interest, no simple method exists to gain insights into their cellular concentrations in a single step. We show that a simple $^1$H NMR experiment can simultaneously measure oxidized and reduced forms of nicotinamide adenine dinucleotide ($NAD^+$ and NADH), oxidized and reduced forms of nicotinamide adenine dinucleotide phosphate ($NADP^+$ and NADPH), and adenosine triphosphate (ATP) and its precursors, adenosine diphosphate (ADP) and adenosine monophosphate (AMP), using mouse heart, kidney, brain, liver, and skeletal muscle tissue extracts as examples. Combining 1D/2D NMR experiments, chemical shift libraries, and authentic compound data, reliable peak identities for these coenzymes have been established. To assess this methodology, cardiac NADH and $NAD^+$ ratios/pool sizes were measured using mouse models with a cardiac-specific knockout of the mitochondrial Complex I *Ndufs4* gene (cKO) and cardiac-specific overexpression of nicotinamide phosphoribosyltransferase (cNAMPT) as examples. Sensitivity of $NAD^+$ and NADH to cKO or cNAMPT was observed, as anticipated. Time-dependent investigations showed that the levels of NADH and NADPH diminish by up to ~50% within 24 h; concomitantly, $NAD^+$ and $NADP^+$ increase proportionately; however, degassing the sample and flushing the sample tubes with helium gas halted such changes. The analysis protocol along with the annotated characteristic fingerprints for each coenzyme is provided for easy identification and absolute quantification using a single internal reference for routine use. The ability to visualize the ubiquitous coenzymes fundamental to cellular functions, simultaneously and reliably, offers a new avenue to interrogate the mechanistic details of cellular function in health and disease.

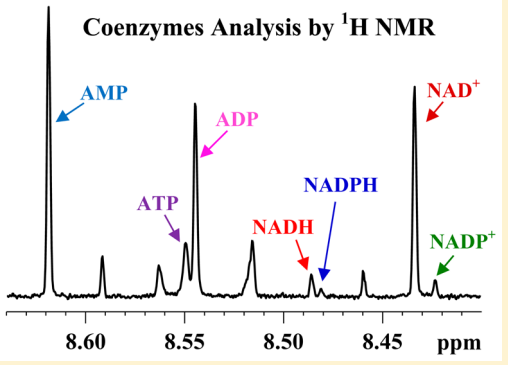


Important coenzymes $NAD^+$ (nicotinamide adenine dinucleotide, oxidized), NADH (nicotinamide adenine dinucleotide, reduced), $NADP^+$ (nicotinamide adenine dinucleotide phosphate, oxidized), and NADPH (nicotinamide adenine dinucleotide phosphate, reduced) mediate biochemical reactions fundamental to cellular functions in health and disease. These coenzymes undergo reversible oxidation and reduction in numerous electron-transfer reactions, while the concentration ratios of the reduced and oxidized forms reflect important cellular functions, including the overall redox status and regulation of ion channels, cell signaling, cell survival, and death.[1−4] This balance is also an important indicator of normal and pathological conditions including heart disease, diabetes, and cancer. Investigations into the metabolism and function of these coenzymes are therefore of immense interest for uncovering fundamental cellular properties, including the slowing of aging processes and treatment of diseases.[3,5,6]

The coenzyme adenosine triphosphate (ATP) is considered to be the energy currency of living cells as it fuels a large number of energy-dependent biochemical processes. Adenosine diphosphate (ADP) and adenosine monophosphate (ADP) are closely associated with ATP as its precursors/products; hence, the levels of ATP, ADP, and AMP represent a measure of the energetics of the functioning cells and their mitochondria.[7] Reliable and high-throughput measurement of the coenzymes of redox reactions and energy, therefore, is important for investigations focused on the mechanistic understanding of normal and impaired cellular functions.[8]

A limited number of analytical methods exist to reliably and simultaneously measure the levels of these coenzymes. Currently, the most often-used methods involve enzymatic assays, which are suboptimal as they necessitate separate protocols for analysis of each coenzyme or their ratios.[9−12] In addition, these assays are often met with challenges due to confounding factors such as interference from other substances in the sample matrix and the finite linear range of the assays. Separately, efforts have been made to simultaneously analyze the coenzymes based on chromatographic separation and UV−vis

**Received:** February 1, 2016
**Accepted:** April 4, 2016
**Published:** April 4, 2016

  

DOI: 10.1021/acs.analchem.6b00442
*Anal. Chem.* 2016, 88, 4817−4824

absorption[13] or detection using targeted mass spectrometry (MS).[14,15] While targeted MS typically provides highly sensitive and robust detection, ion suppression and peak interference make reliable quantification of these coenzymes challenging. For example, $NAD^+$ and $NADP^+$ can overlap with NADH and NADPH, respectively, due to their unit mass differences. In addition, in-source fragmentation of ATP and ADP to AMP poses a major challenge for reliable analysis of these compounds using MS.[15]

Nuclear magnetic resonance (NMR) spectroscopy offers numerous benefits, including the ability to reliably identify and simultaneously quantify many compounds in complex biological mixtures with high reproducibility and quantification accuracy.[16−21] To date, owing to NMR's ability to detect and quantify metabolites in vivo, the coenzymes, $NAD^+$, NADH, and ATP, along with ADP and AMP, have been measured directly or indirectly utilizing in vivo $^{31}P$ NMR.[22−24] More recently, a method to measure $NAD^+$ in the rat brain has been shown using in vivo $^1H$ NMR.[25] The ability to analyze the coenzymes in vivo is attractive as it promises better insights; currently, however, the limited resolution and sensitivity due to many factors such as chemical shift anisotropy, dipolar, and quadrupolar interactions, and changes in magnetic susceptibility, deleteriously affect reliable and simultaneous analysis of the coenzymes by this approach. In the case of $^1H$ detection in vivo, the need to suppress the abundant water signal adds to the challenges.

Ex vivo NMR, on the other hand, alleviates many challenges associated with in vivo NMR and provides highly resolved spectra to enable routine quantification of metabolites down to submicromolar concentrations using a single internal reference.[26] To detect the coenzymes, it is necessary to establish their characteristic fingerprints and, in particular, isolated peaks that can be used for quantification on a routine basis. The complexity of biological mixtures combined with the instability of coenzymes, their virtually identical structures, and low concentrations has so far prevented reliable measurement of the coenzymes by NMR. In the current study, we have overcome this bottleneck and provide a simple NMR method to quantify the coenzymes simultaneously. The outcome is based on comprehensive investigations of a variety of mouse tissues using both 1D and 2D NMR spectroscopy methods, the development and use of a NMR chemical shift library and tissue harvesting and extraction method, and spiking with authentic compounds. As a result, the simultaneous and facile quantification of seven major coenzymes along with many other metabolites is demonstrated, using knockout and transgenic mouse models as examples.

## MATERIALS AND METHODS

Methanol, chloroform, monosodium phosphate ($NaH_2PO_4$), disodium phosphate ($Na_2HPO_4$), sodium salt of 3-(trimethylsilyl)-propionic acid-2,2,3,3-$d_4$ (TSP), potassium hydroxide, and perchloric acid were obtained from Sigma-Aldrich (St. Louis, MO). Standard compounds used for chemical shift data and/or spiking experiments were all obtained from Sigma-Aldrich or Fisher (Waltham, MA), except for the coenzymes, $NAD^+$, NADH, $NADP^+$, and NADPH, which were generously provided by Dr. Jianhai Du, University of Washington (Table S1). Deuterium oxide ($D_2O$) was obtained from Cambridge Isotope laboratories, Inc. (Andover, MA). Deionized (DI) water was purified using an in-house Synergy Ultrapure Water System from Millipore (Billerica, MA). All chemicals were used without further purification.

**Solutions of Authentic Compounds for Spiking Experiments/Chemical Shift Database.** One milliliter stock solutions (1 mM) for standard compounds (Table S1) were prepared in $D_2O$ by diluting their 50 mM solutions, which were first prepared by weighing each compound and dissolving it in $D_2O$. A 60 $\mu$L solution of each compound was mixed with 540 $\mu$L phosphate buffer (0.1 M; pH = 7.45) in $D_2O$ containing 50 $\mu$M TSP to obtain solutions of 100 $\mu$M concentration, which were then transferred to 5 mm NMR tubes.

**Mouse Tissue Separation and Extraction.** The investigations using mouse tissue were performed with the approval of the Institutional Animal Care and Use Committee of the University of Washington. After each mouse was anesthetized, heart, kidney, brain, liver, and skeletal muscle tissues were separated, rinsed in cold phosphate-buffered saline (PBS), and snap frozen in liquid nitrogen (Table S2). Different tissue harvesting and extraction methods were tested for the mouse heart tissue to determine the optimal method for the targeted coenzymes. The tissue harvesting procedures employed included: freeze clamping after 20 min of Langendorff isolated heart perfusion[27] and freeze clamping separated hearts after washing with a solution in which glucose (10 mM) and pyruvate (0.5 mM) were present or in cold PBS.

The extraction procedures included the use of a mixture of methanol and water, perchloric acid (0.6 N), or methanol and chloroform. For methanol and water extraction, weighed tissue specimens were mixed with 200 $\mu$L cold water and methanol (1:5 v/v; 4 °C) in 2 mL Eppendorf vials and homogenized using a Tissue-Tearor hand-held homogenizer. A further 800 $\mu$L cold water/methanol solution (1:5 v/v) was added, each mixture was then vortexed and incubated on dry ice (−75 °C) for 30 min. Subsequently, the mixtures were sonicated in an ice bath for 10 min and centrifuged for 5 min at 2039 rcf and low temperature (4 °C). The soluble extracts were separated, frozen using dry ice, and then lyophilized to dryness.

For perchloric acid extraction, weighed tissue specimens were mixed with 400 $\mu$L cold 0.6 N perchloric acid (4 °C) in 2 mL Eppendorf vials and homogenized using Tissue-Tearor hand-held homogenizer. Cold distilled water (400 $\mu$L) was added, and each mixture was then vortexed and incubated on dry ice (−75 °C) for 30 min. Subsequently, the mixtures were sonicated in an ice bath for 10 min and centrifuged for 5 min at 2039 rcf and low temperature (4 °C). The soluble extracts were separated, neutralized using potassium hydroxide, and the insoluble residue was pelleted by centrifugation for 5 min at 2039 rcf (4 °C). The soluble extracts were frozen using dry ice and lyophilized to dryness.

For methanol and chloroform extractions, weighed tissue specimens (~5 to 80 mg) were mixed with a 1 mL mixture of cold methanol and chloroform (1:2 v/v; 4 °C) in 2 mL Eppendorf vials and homogenized using a Tissue-Tearor hand-held homogenizer and sonicated for 20 s. A further 800 $\mu$L cold chloroform/distilled water mixture (1:1 v/v) was added, the sample was then vortexed and set aside for 30 min on ice to separate the solvent layers. Next, after centrifugation at 2039 rcf, the aqueous (top) layer was separated and filtered using 1.5 mL 0.2 $\mu$m syringe filters and freeze-dried. To test the extraction method using recovery experiments, a small set of heart tissue samples ($n$ = 6) were extracted with or without spiking with a standard mixture of the coenzymes. The dried extracts were mixed with 210 or 600 $\mu$L of a cold phosphate


DOI: 10.1021/acs.analchem.6b00442
Anal. Chem. 2016, 88, 4817−4824

Table 1. $^1$H NMR Chemical Shifts (in ppm) and $J$ couplings (in Hz) for the Coenzymes/Metabolites of Redox Reaction and Cellular Energy

| coenzyme/metabolite | mouse heart/kidney/brain/liver/skeletal muscle | authentic compounds[b] |
|---|---|---|
| nicotinamide adenine dinucleotide, oxidized ($NAD^+$) | 4.371 (m); 4.387 (m); 4.429 (m); 4.487 (t, $J$ = 5.213); 4.515 (m); 4.545 (m); 6.041[a] (1H, d, $J$ = 6.042); 6.093[a] (1H, d, $J$ = 5.482); 8.174[a] (1H, s); 8.193[a] (1H, dd); 8.434[a] (1H, s); 8.832[a] (1H, d, $J$ = 7.992); 9.147[a] (1H, d, $J$ = 6.158); 9.344[a] (1H, s) | 4.191−4.291 (m); 4.369 (m); 4.386 (m); 4.430 (m); 4.488 (t; $J$ = 5.196); 4.514 (m); 4.546 (m); 6.042 (d, $J$ = 6.089); 6.092 (d, $J$ = 5.510); 8.176 (s); 8.193 (dd); 8.435 (s); 8.833 (d; $J$ = 8.032); 9.148 (d; $J$ = 6.138); 9.344 (s) |
| nicotinamide adenine dinucleotide phosphate, oxidized ($NADP^+$) | 6.101 (d); 8.146[a] (1H, s), 8.424[a] (1H, s); 9.104[a] (1H, d); 9.300[a] (1H, s) | 4.181−4.236 (m); 4.284−4.342 (m); 4.377 (m); 4.411 (m); 4.461 (t; $J$ = 5.286); 4.503 (m); 4.617 (t, $J$ = 4.990); 4.968 (m); 6.037 (d; $J$ = 5.560); 6.101 (d, $J$ = 4.969); 8.146 (s); 8.168−8.199 (m); 8.423 (s); 8.818 (d, $J$ = 8.008); 9.106 (d; $J$ = 6.259); 9.299 (s) |
| nicotinamide adenine dinucleotide, reduced (NADH) | 6.137 (d); 6.942[a] (1H, s); 8.247[a] (1H, s); 8.486[a] (1H, s) | 2.669 (br. d, $J$ = 17.976); 2.793 (br. d, $J$ = 17.976); 4.082 (br. m); 4.097 (br. m) 4.169−4.289 (br. m); 4.389 (br. m); 4.512 (t, $J$ = 4.448); 4.709 (t, $J$ = 5.272); 5.980 (d, $J$ = 8.424); 6.138 (d, $J$ = 5.479); 6.943 (s); 8.248 (s); 8.487 (s) |
| nicotinamide adenine dinucleotide phosphate, reduced (NADPH) | 6.216 (d); 6.936[a] (1H, s); 8.481[a] (1H, s) | 2.737 (br. d, $J$ = 18.093); 2.838 (br. d, $J$ = 18.093); 4.044 (br. m); 4.066 (br. m); 4.154−4.236 (m); 4.285−4.325 (br. m); 4.390 (br. m); 4.597 (t, $J$ = 5.049); 4.950 (m); 5.963 (d, $J$ = 8.363); 6.216 (d, $J$ = 4.597); 6.935 (s); 8.246 (s); 8.481 (s) |
| adenine triphosphate (ATP) | 4.410 (m); 4.621(m); 6.155 (d); 8.274 (s); 8.549[a] (1H, s) | 4.192−4.233 (m); 4.278−4.318 (m); 4.392−4.421 (br. m); 4.620−4.648 (m); 6.153 (d, $J$ = 5.974); 8.274 (s); 8.557 (s) |
| adenine diphosphate (ADP) | 4.387 (m); 4.621(m); 6.155 (d); 8.273 (s); 8.544[a] (1H, s) | 4.187−4.219 (m); 4.244−4.283 (m); 4.377−4.398 (br. m); 4.611−4.634 (m); 6.156 (d, $J$ = 5.383); 8.273 (s); 8.547 (s) |
| adenine monophosphate (AMP) | 4.014 (m); 4.372 (m); 4.515 (m); 6.147 (d); 8.271 9(s); 8.619[a] (1H, s) | 3.995−4.026 (m); 4.359−4.383 (br. m); 4.501−4.526 (m); 6.148 (d, $J$ = 5.965); 8.272 (s); 8.620 (s) |

[a]Chemical shifts for characteristic peaks of metabolites that provide unambiguous information for identification and quantification using 1D $^1$H NMR. Chemical shifts for authentic compounds are also shown separately for comparison. [b]Spectra for the authentic compounds were obtained near their physiological concentrations (100 $\mu$M) in $D_2O$ buffer at pH 7.45 at 298 K. Abbreviations: br. broad; s, singlet; d, doublet; dd, doublet of doublets; t, triplet; m, multiplet.

buffer (0.1 M; pH = 7.45; 4 °C) in $D_2O$ containing 25 or 50 $\mu$M TSP. The solutions were transferred to sample tubes for measurements; 3 mm sample tubes were used for 210 $\mu$L solutions, and 5 mm sample tubes were used for 600 $\mu$L solutions.

**NMR Spectroscopy.** Experiments for a few tissue samples were performed at different temperatures (280, 290, and 298 K) to ensure that stability of the coenzymes was not affected by their analysis at room temperature. Subsequently, all NMR experiments were performed at 298 K. A Bruker Avance III 800 MHz spectrometer equipped with a cryogenically cooled probe and $z$-gradients suitable for inverse detection was used. A few experiments were performed on a Bruker Avance III 700 MHz spectrometer equipped with a room temperature probe and $z$-gradients suitable for inverse detection. The one-pulse or 1D NOESY pulse sequence with residual water suppression using presaturation, 10204 Hz (for 800 MHz) or 11160 Hz (for 700 MHz) spectral width, 6.6 s recycle delay, 128 transients, and 32 K time domain points were used for $^1$H 1D NMR experiments. For tissue extracts, NMR experiments were performed immediately after preparing the solutions and a second time 24 h after preparing the solutions to also assess the stability of the redox coenzymes. Separately, NMR experiments were also performed using degassed NMR solvent ($D_2O$ buffer), and sample tubes flushed with helium gas to test whether oxidation of NADH/NADPH to $NAD^+$/$NADP^+$ could be prevented. After degassing, the sample tubes were sealed using parafilm, and experiments were performed immediately after preparing the solutions and a second time 24 h after preparing the solutions. To aid identification, homonuclear two-dimensional (2D) experiments, such as $^1$H−$^1$H double quantum filtered correlation spectroscopy (DQF-COSY) and $^1$H−$^1$H total correlation spectroscopy (TOCSY) experiments, were performed at 800 MHz for all types of tissue specimens, in addition to the 1D NMR experiments. The 2D experiments were performed with suppression of the residual water signal by presaturation during the relaxation delay. A sweep width of 9600 Hz was used in both dimensions; 512 or 400 FIDs were obtained with $t_1$ increments for DQF-COSY or TOCSY, respectively, each with 2048 complex data points. The number of transients used was 8 or 16 for DQF-COSY and 8, 16, or 24 for TOCSY. The relaxation delay was 2.0, 2.2, or 2.5 s for DQF-COSY and 1.0, 1.3, or 1.5 s for TOCSY. The resulting 2D data were zero-filled to 1024 points in the $t_1$ dimension. A 90° shifted squared sine-bell window function was applied to both dimensions before Fourier transformation. To confirm the assigned peaks, spectra were also obtained before and after addition of 10−20 $\mu$L stock solutions (1 mM) of authentic coenzymes to the tissue extract solutions. Chemical shifts were referenced to the internal TSP signal for both the $^1$H 1D and 2D spectra. Bruker Topspin versions 3.0 or 3.1 software packages were used for NMR data acquisition, processing, and analyses.

**Peak Assignments, Coenzyme Identification, and Quantification.** Initial peak assignments relied on database searches,[28−30] including the human metabolome database (HMDB)[28] and the biological magnetic resonance data bank (BMRB).[29] However, unambiguous identification of the coenzymes necessitated the development of a new chemical shift database consisting of the coenzymes and other compounds in solutions at concentrations similar to their levels in tissue (Table 1). Spectral peaks for all the coenzymes were identified using this database along with peak multiplicity, $J$ coupling measurements, and the comprehensive analyses of



DOI: 10.1021/acs.analchem.6b00442
Anal. Chem. 2016, 88, 4817−4824

2D DQF-COSY and TOCSY spectra. The coenzymes thus identified were further confirmed by spiking experiments using authentic compounds. Chenomx NMR Suite Professional (version 5.1; Chenomx Inc., Edmonton, Alberta, Canada) was used to quantify the coenzyme peaks. Chenomx allows fitting spectral lines using the standard metabolite library for 800 MHz $^1$H NMR spectra, and in particular, the determination of concentrations. Since the proximity of chemical shift values for signals from multiple compounds resulted in the software providing multiple library hits for the same peak, the correct identification of coenzymes' peaks relied on the newly established peak assignments. Peak fitting with reference to the internal TSP signal enabled the determination of absolute concentrations of the coenzymes.

## RESULTS AND DISCUSSION

The $^1$H NMR spectra from mouse tissues are complex, with a large number of highly resolved peaks (Figure 1a), and the spectrum for each tissue type, namely, liver, heart, kidney, brain, and skeletal muscle, is distinct (Figure S1). Specifically, the region from ~0.5 to 6.3 ppm is more complex due to contributions from many small molecule metabolites when compared to the relatively sparse region from ~6.5 to 9.5 ppm. On the basis of their structures and the available chemical shift databases of authentic compounds,[28−30] the coenzymes were anticipated to have peaks in both regions of the spectra (Table 1). Using the chemical shift database that we have newly developed and comprehensive analyses of 1D and 2D NMR data, unambiguous identification of the coenzymes, $NAD^+$, NADH, $NADP^+$, NADPH, and ATP, along with ADP and AMP, in all the types of tissue samples were made. NMR peaks from the coenzymes that appear below 6.3 ppm were largely overlapped with each other and with peaks from other compounds. The region between 6.5 to 9.5 ppm, on the other hand, was dominated by peaks from the coenzymes, and each coenzyme showed one or more well-resolved peaks (Figure 1b and Figure S2). Of particular interest is the narrow spectral region between 8.4 to 8.64 ppm; it showed a characteristic, well-resolved peak for each coenzyme for all the types of tissue studied (Figure 1c and 2). Each of these characteristic signals

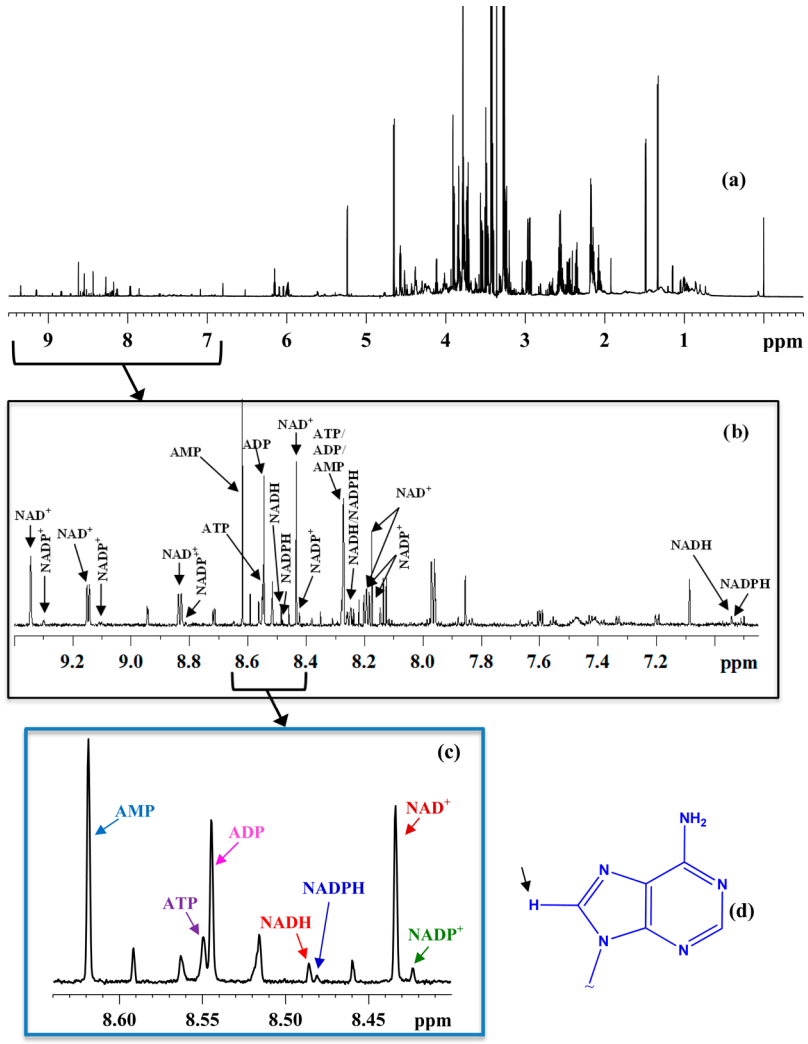


**Figure 1.** (a) Typical 800 MHz $^1$H NMR spectrum of a mouse liver tissue extract obtained using a 5 mm sample tube; (b) expanded spectral region with annotations for peaks for oxidized nicotinamide adenine dinucleotide ($NAD^+$), oxidized nicotinamide adenine dinucleotide phosphate ($NADP^+$), reduced nicotinamide adenine dinucleotide (NADH), reduced nicotinamide adenine dinucleotide phosphate (NADPH), adenosine triphosphate (ATP), adenosine diphosphate (ADP), and adenosine monophosphate (AMP); (c) expanded spectral region showing the characteristic fingerprint of the redox and energy coenzymes; and (d) adenine moiety with the lone hydrogen atom on the five-membered ring indicated by an arrow; coenzymes peaks in the fingerprint region shown in (c) arise from this hydrogen atom (see also Figure S3).



DOI: 10.1021/acs.analchem.6b00442
*Anal. Chem.* 2016, 88, 4817−4824

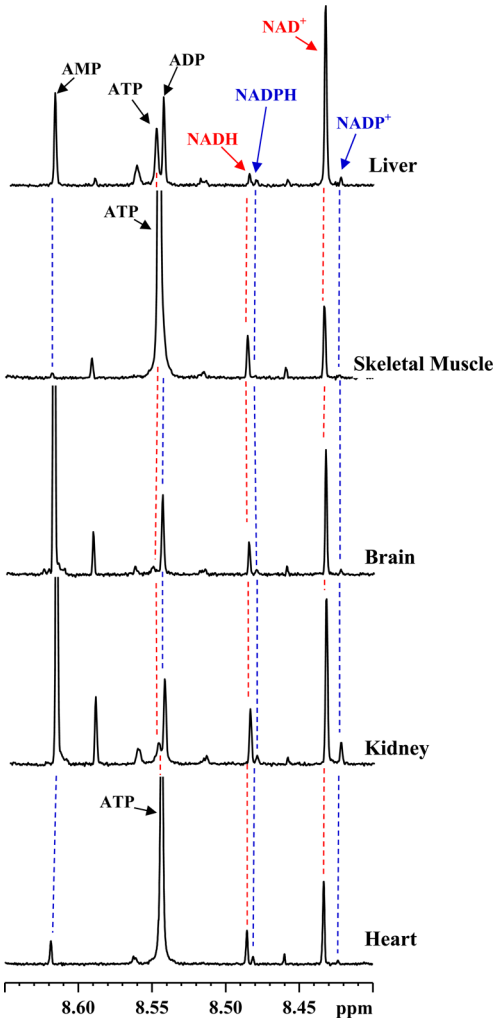


**Figure 2.** Characteristic annotated fingerprint regions of 800 MHz $^1$H NMR spectra of a mouse heart, kidney, brain, skeletal muscle, and liver tissue extracts for visualization and simultaneous quantification of the coenzymes. A three millimeter sample tube was used for the heart tissue, and 5 mm sample tubes were used for others.

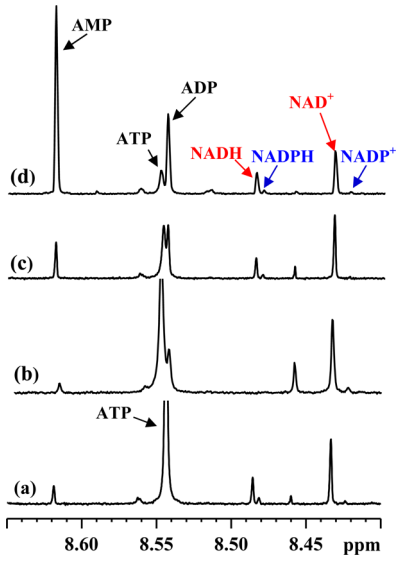


**Figure 3.** Portions of 800 MHz $^1$H NMR spectra obtained using 3 mm sample tubes highlighting the sensitivity of coenzyme levels to tissue harvesting/extraction protocols: (a) mouse heart harvested, washed with glucose/pyruvate solution and freeze clamped, followed by extraction using methanol-chloroform mixture; (b) mouse heart harvested, perfused with glucose/pyruvate solution and freeze clamped, followed by extraction using methanol-chloroform mixture; (c) mouse heart freeze clamped in vivo, followed by extraction using methanol-chloroform mixture; and (d) mouse heart harvested, washed with PBS and freeze clamped, followed by extraction using methanol−water mixture. Of the prominent changes are the missing NADH/NADPH peaks in (b) and diminished ATP and enhanced ADP/AMP in (c, d).

arises from the same lone proton of the five-membered ring of the adenine moiety (Figure 1d and Figure S3).

Considering the challenges associated with the analysis of the coenzymes using current methods, the benefits offered by NMR spectroscopy as an alternative and simple approach are striking. A major limiting factor for NMR to date, however, has been the inability to obtain reproducible NMR spectra due to the unstable nature of many coenzymes and challenges related to sample preparation (Figure 3), as well as a lack of knowledge regarding their unambiguous identification. The high spectral complexity of the coenzymes, their similarity in structure, the sensitivity of chemical shifts to parameters such as concentration, pH, and ionic strength, and the low concentration, specifically, for some of the coenzymes have made their unambiguous identification in NMR spectra difficult. For example, due to the structural similarity, NMR peaks for some of the coenzymes are virtually indistinguishable. In particular, the separation between the characteristic $C_8$-proton peaks for NADH and NADPH is only 0.004 ppm (3.2 Hz) due to their virtually identical structures (Figure S3). ATP and ADP also exhibit similar peak characteristics (Figure 1c and Table 1). The sensitivity of the chemical shift to numerous parameters such as concentration, pH, ionic strength, and temperature can cause the closely spaced peaks for several coenzymes to interchange their peak positions in the chemical shift databases of authentic compounds.[28,29] To circumvent this problem, in this study, we developed a unique NMR chemical shift library for the coenzymes by maintaining their concentrations similar to their physiological levels in the tissue extracts, and using solvent, pH, and temperature conditions identical to those used for the tissue samples (Table 1). Combining this coenzyme chemical shift database with peak multiplicity and J-couplings, as well as comprehensive analysis using a series of 1D and 2D DQF-COSY and TOCSY spectra, characteristic peaks for the coenzymes were unambiguously identified. Finally, the identified coenzymes were further confirmed by spiking using authentic compounds.

For absolute quantification using NMR, the establishment of the identity of at least one isolated peak for each coenzyme is critical, and the 8.4 to 8.64 ppm region fulfills this requirement (Figure 1c). Fortuitously, within this fingerprint, none of the tissue types exhibited any interference from other compounds. Furthermore, and importantly, the peaks for the coenzymes in the fingerprint region are all singlets, as they all arise from the lone hydrogen atom on the five-membered ring of the adenine moiety, which is very useful because it provides the best resolution and sensitivity compared to peak multiplets. This is particularly critical for identifying the coenzymes that are very closely spaced and exhibit concentrations of a few ng/mg tissue. Another useful characteristic of the fingerprint region shown in Figure 1c and Figure 2 is that ratios between various coenzymes can be visualized directly and simultaneously from their peak heights without resorting to any calculations, owing to the fact that each coenzyme's peak is represented by a single hydrogen atom (Figure S3).


DOI: 10.1021/acs.analchem.6b00442
Anal. Chem. 2016, 88, 4817−4824

In general, numerous peaks observed for each coenzyme in different regions of the same spectra (Table 1 and Figures S1, S2 and S4) serve to verify their identities, unambiguously, and determine their concentrations, reliably. In particular, it may be noted that ambiguity may arise for distinguishing between ATP and ADP when their peaks overlap or the ATP peak drifts to low frequency toward the ADP peak as for the heart and skeletal muscle tissues shown in Figures 2 and 3. Such a situation arises especially when the peak intensity for one of the compounds is overwhelmingly high compared to the other. In such a case, unambiguous identification and reliable quantification of ATP and ADP is achieved in combination with other peaks that appear in different parts of the same spectra that do not overlap with each other. For example, the spectral region that satisfies this condition is between ~4.1 and 4.5 ppm, in which peaks for ATP are well-isolated from ADP as illustrated in the Figure S4.

It is important to note that the coenzymes such as NADH, NADPH, and ATP are extremely labile, and they can evade detection wholly or partly depending on the procedure used for tissue harvesting/extraction. Using mouse hearts, we evaluated numerous different tissue harvesting/extraction protocols to assess their effects on the detection of the coenzymes. As seen in Figure 3, widely varying results were obtained for different harvesting/extraction conditions. Quickly washing the harvested tissue with a solution containing glucose and pyruvate and freeze clamping, followed by extraction using a mixture of methanol and chloroform provided the best results in terms of peak areas/concentrations of the detected coenzymes (Figure 3a). Notably, the other protocols resulted in a significant or complete loss of NADH and NADPH (Figure 3b) or ATP (Figure 3, panels c and d). Subsequent investigations for heart tissue, in this study, utilized the optimized protocol as shown for Figure 3a. The robustness of the extraction method can be visualized from results of a recovery test made by adding a mixture of standard compounds (Table S3). It may be noted that, as shown in Figure 2, kidney, brain, and liver tissue exhibited a significant loss of ATP signals and gain of ADP and AMP signals. These changes are likely to be due to the fact that tissue from kidney, brain, and liver were obtained from the same mouse after the heart was separated. Interestingly, however, although the skeletal muscle was obtained last, it did not exhibit such changes (Figure 2).

On the basis of the now established peak identity for each coenzyme and an optimal harvesting/extraction protocol for mouse heart tissue (Figure 3a), concentrations of the redox coenzymes, $NAD^+$, NADH, $NADP^+$, and NADPH were measured using Chenomx. Simultaneously, concentrations of ATP, ADP, and AMP were also measured using the same spectra. Typical concentrations thus obtained for mouse heart tissue are shown in Figure 4. Next we employed mouse models with disturbed NAD(H) redox balance to test the efficacy of this approach. Cardiac-specific *Ndufs4* knockout (cKO) mice present inhibited mitochondrial Complex I activity.[31] We observed an increase in NADH and the NADH/$NAD^+$ ratio with little change in the NADH/$NAD^+$ pool in cKO hearts compared to wild-type (WT) (Figure 5). In contrast, the transgenic mice that overexpress nicotinamide phosphoribosyltransferase

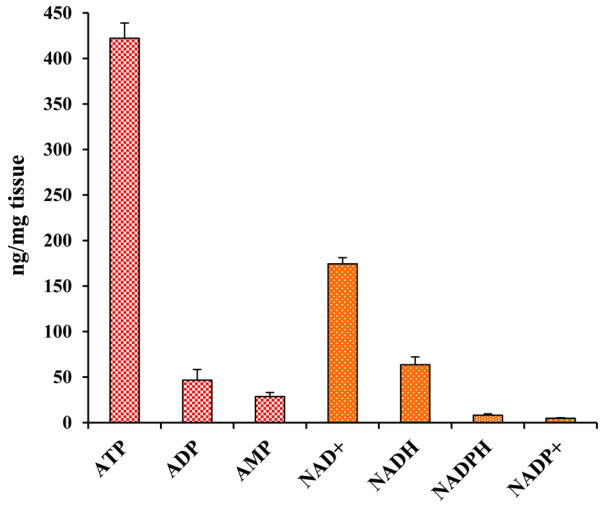


**Figure 4.** Absolute concentrations for ATP, ADP, AMP, $NAD^+$, NADH, $NADP^+$, and NADPH in heart tissue of wild type mice ($n = 6$) obtained in a single step using the $^1$H NMR spectroscopy method.

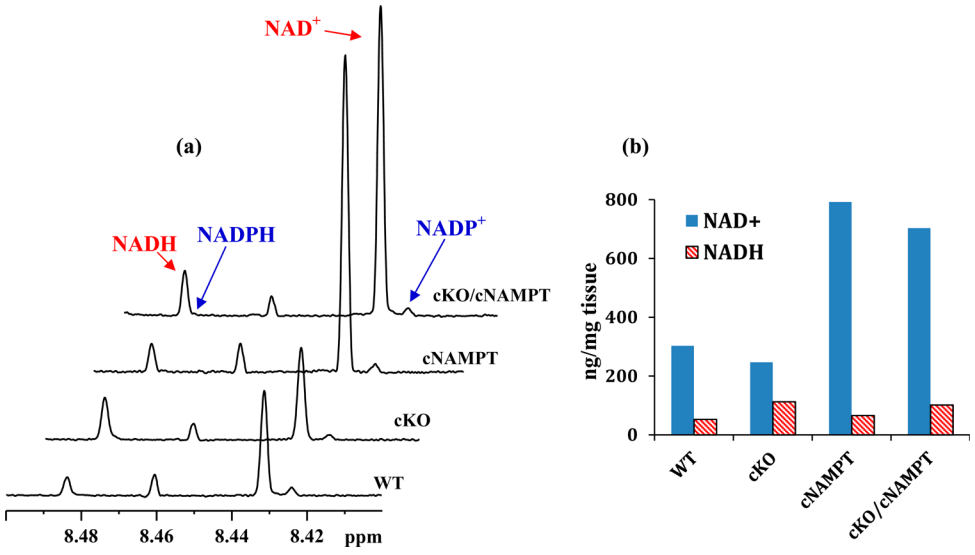


**Figure 5.** (a) Portions of typical 800 MHz NMR spectra of heart tissue extracts obtained using 3 mm sample tubes highlighting the changing $NAD^+$ and NADH peaks' intensity in WT, cKO, cNAMPT, and cKO/cNAMPT mice and (b) the corresponding concentrations (ng/mg) in the cardiac tissues shown in (a).



DOI: 10.1021/acs.analchem.6b00442
*Anal. Chem.* 2016, 88, 4817−4824

(cNAMPT) only in hearts[32] exhibited elevated $NAD^+$ levels and NAD(H) pool size. In addition, cKO mice with cNAMPT expression showed higher $NAD^+$ levels as well as NAD(H) pool size but lower NADH/$NAD^+$ ratios than those in cKO mice (Figure 5b). These changes are illustrated in Figure 5a as portions of representative NMR spectra highlighting the $NAD^+$ and NADH peaks for different genetic variants and the corresponding concentrations shown in Figure 5b. The results from cKO and cNAMPT hearts are consistent with the literature[31,32] and indicate that the new approach will be a useful tool to the investigations of a number of diseases.

More generally, this approach is applicable for all tissue types and enables absolute quantification of the seven coenzymes including the NAD(H) and NADP(H) redox couples in a single experiment, which is important to assess the biological significance of their levels in health and disease. In contrast, the established enzymatic assays increase the likelihood of errors due to the requirement of separate sample preparation steps for their measurement, individually. Further, because the NMR approach offers the ability to see each coenzyme peak with the naked eye, it offers a new avenue to evaluate the quality of extraction, simultaneously, which is critical considering the sensitivity of many coenzymes to the extraction protocol used (Figure 3).

Using the NMR approach, the time and temperature dependences of the coenzymes were evaluated to assess their stability in solution. The results show that apart from small chemical shift changes, the coenzymes did not show any effect of temperature in the range of 280−298 K. Hence, 298 K was chosen for investigations in this study. Time-dependent analysis, however, showed that the levels of the reduced forms of the coenzymes, NADH and NADPH, decreased with time and the levels of their oxidized forms, $NAD^+$ and $NADP^+$, increased, proportionately. Over a period of 24 h after preparation of the solutions, roughly 50% or more of the NADH and NADPH levels were reduced (Figure S5). Interestingly, however, degassing the NMR solvent and flushing the sample tube with helium gas, followed by sealing the tube with Parafilm, prevented such a change (Figure S6). These results indicate the somewhat unstable nature of NADH and NADPH in solution in the presence of oxygen and highlight the need to analyze the samples as soon as the solutions are made, or otherwise degas the solvent and the sample tube using an inert gas.

In this study, about 5 to 80 mg tissue was used to develop the NMR method for simultaneous analysis of the coenzymes within a 10 to 15 min analysis time. The phosphorylated redox coenzymes $NADP^+$ and NADPH, which are generally found at much lower concentrations (a few ng/mg tissue) compared to the other coenzymes, benefit from using large amount of tissue. On the basis of the results, however, the other coenzymes with larger signals (typically 10-fold, Figure 4) can be quantified using <10 mg tissue (Figure S7). Further, utilizing sensitivity enhancement approaches, such as with additional signal averaging or utilizing microcoil probes, the detection limit can be reduced further to enable the analysis of smaller amounts of biological samples (<5 mg) for absolute concentrations of all the coenzymes.

In conclusion, we demonstrate a simple method for the simultaneous quantification of the major coenzymes of cellular energy and redox reactions: $NAD^+$, NADH, $NADP^+$, NADPH, and ATP along with ADP and AMP using $^1$H NMR spectroscopy. Considering that the balance between the redox coenzymes play critical roles in various cellular functions, their involvement in electron shuttling in oxidation reduction reactions,[5] and the challenges associated with the established analysis methods, the ability of an NMR method to visualize cellular levels of the coenzymes represents a significant step for mechanistic understanding of cellular metabolism in health and disease. A one-step detection of the coenzymes is demonstrated for different types of mouse tissue with the goal of evaluating the utility of the method for a wide range of biological specimens. As an example of the utility of this method, the sensitivity of coenzymes $NAD^+$ and NADH to different mouse tissue genotypes is demonstrated. Experimental protocols along with the annotated spectral fingerprints of the coenzymes provided here enable their easy identification and simultaneous quantification using a single internal reference. An added advantage of this method is that it not only enables analysis of the coenzymes but also enables analysis of a large number of other small molecule metabolites, simultaneously, from the same NMR data without the need for additional sample or experiments (Figure S8), as we have demonstrated recently for human blood.[26] The time-dependent studies indicate the gradual oxidation of NADH and NADPH to $NAD^+$ and $NADP^+$, respectively, in solution at room temperature, which points to the need to analyze them as soon as the solutions are made. Alternatively, degassing the NMR solution and flushing the NMR tubes using an inert gas such as helium, followed by sealing the tube, can provide reliable quantification. This is the first successful effort providing the absolute quantification of major coenzymes of cellular redox reactions and cellular energy, simultaneously, and this approach is anticipated to find widespread utility for investigations of cellular function.

## ■ ASSOCIATED CONTENT

### Supporting Information

The Supporting Information is available free of charge on the ACS Publications website at DOI: 10.1021/acs.analchem.6b00442.

List of metabolites used for spiking total number and type of mice used in the study, results of recovery test performed using mouse heart tissue and optimized extraction protocol, additional $^1$H NMR spectra, and structures identifying NMR peaks in fingerprint region (PDF)

## ■ AUTHOR INFORMATION


### Corresponding Authors

*E-mail: ngowda@uw.edu.
*E-mail: draftery@uw.edu.


### Notes

The authors declare the following competing financial interest(s): Daniel Raftery reports holding equity and an executive position at Matrix Bio, Inc.

## ■ ACKNOWLEDGMENTS

The authors gratefully acknowledge financial support from the National Institutes of Health Grants GM085291, HL118989, HL110349, P30DK035816, and NIH/NIBIB T32EB1650, and from the American Heart Association Grant 13POST16200007.

## ■ REFERENCES


(1) Kilfoil, P. J.; Tipparaju, S. M.; Barski, O. A.; Bhatnagar, A. *Circ. Res.* **2013**, *112* (4), 721−41.
(2) Koch-Nolte, F.; Haag, F.; Guse, A. H.; Lund, F.; Ziegler, M. *Sci. Signaling* **2009**, *2* (57), mr1.
(3) Ying, W. *Antioxid. Redox Signaling* **2008**, *10* (2), 179−206.




DOI: 10.1021/acs.analchem.6b00442
*Anal. Chem.* 2016, 88, 4817−4824

(4) Engel, P. C. *Neurochem. Res.* **2014**, *39* (3), 426−32.
(5) Nakamura, M.; Bhatnagar, A.; Sadoshima, J. *Circ. Res.* **2012**, *111* (5), 604−10.
(6) Oka, S.; Hsu, C. P.; Sadoshima, J. *Circ. Res.* **2012**, *111* (5), 611−27.
(7) Nelson, D. L.; Cox, M. M. *Lehninger Principles of Biochemistry*, 6th ed.; Freeman & Company, W. H.: New York, 2012.
(8) Bar-Or, D.; Bar-Or, R.; Rael, L. T.; Brody, E. N. *Redox Biol.* **2015**, *4*, 340−345.
(9) Du, J.; Cleghorn, W.; Contreras, L.; Linton, J. D.; Chan, G. C.; Chertov, A. O.; Saheki, T.; Govindaraju, V.; Sadilek, M.; Satrústegui, J.; Hurley, J. B. *Proc. Natl. Acad. Sci. U. S. A.* **2013**, *110* (46), 18501−18506.
(10) Santidrian, A. F.; Matsuno-Yagi, A.; Ritland, M.; Seo, B. B.; LeBoeuf, S. E.; Gay, L. J.; Yagi, T.; Felding-Habermann, B. *J. Clin. Invest.* **2013**, *123* (3), 1068−1081.
(11) Anderson, R. M.; Bitterman, K. J.; Wood, J. G.; Medvedik, O.; Cohen, H.; Lin, S. S.; Manchester, J. K.; Gordon, J. I.; Sinclair, D. A. *J. Biol. Chem.* **2002**, *277*, 18881−18890.
(12) Smith, J. S.; Brachmann, C. B.; Celic, I.; Kenna, M. A.; Muhammad, S.; Starai, V. J.; Avalos, J. L.; Escalante-Semerena, J. C.; Grubmeyer, C.; Wolberger, C.; Boeke, J. D. *Proc. Natl. Acad. Sci. U. S. A.* **2000**, *97*, 6658−6663.
(13) Sporty, J. L.; Kabir, M. M.; Turteltaub, K. W.; Ognibene, T.; Lin, S. J.; Bench, G. *J. Sep. Sci.* **2008**, *31* (18), 3202−3211.
(14) Evans, C.; Bogan, K. L.; Song, P.; Burant, C. F.; Kennedy, R. T.; Brenner, C. *BMC Chem. Biol.* **2010**, *10*, 2.
(15) Trammell, S. A. J.; Brennera, C. *Comput. Struct. Biotechnol. J.* **2013**, *4*, No. e201301012.
(16) Nagana Gowda, G. A.; Zhang, S.; Gu, H.; Asiago, V.; Shanaiah, N.; Raftery, D. *Expert Rev. Mol. Diagn.* **2008**, *8* (5), 617−633.
(17) Larive, C. K.; Barding, G. A., Jr; Dinges, M. M. *Anal. Chem.* **2015**, *87* (1), 133−46.
(18) Halouska, S.; Fenton, R. J.; Barletta, R. G.; Powers, R. *ACS Chem. Biol.* **2012**, *7* (1), 166−171.
(19) Clendinen, C. S.; Lee-McMullen, B.; Williams, C. M.; Stupp, G. S.; Vandenborne, K.; Hahn, D. A.; Walter, G. A.; Edison, A. S. *Anal. Chem.* **2014**, *86* (18), 9242−9250.
(20) Ellinger, J. J.; Chylla, R. A.; Ulrich, E. L.; Markley, J. L. *Curr. Metabolomics* **2012**, *1* (1), 28−40.
(21) Nagana Gowda, G. A.; Raftery, D. *J. Magn. Reson.* **2015**, *260*, 144−60.
(22) Zhu, X. H.; Lu, M.; Lee, B. Y.; Ugurbil, K.; Chen, W. *Proc. Natl. Acad. Sci. U. S. A.* **2015**, *112* (9), 2876−2881.
(23) Ingwall, J. S. *ATP and the Heart*; Kluwer Academic Publishers: Norwell, MA, 2002.
(24) Bottomley, P. A. NMR Spectroscopy of the Human Heart. In *Encyclopedia of Magnetic Resonance*; Harris, R. K., Wasylishen, R. E., Eds.; John Wiley: Chichester, U.K., 2009.
(25) de Graaf, R. A.; Behar, K. L. *NMR Biomed.* **2014**, *27*, 802−809.
(26) Nagana Gowda, G. A.; Gowda, Y. N.; Raftery, D. *Anal. Chem.* **2015**, *87* (1), 706−715.
(27) Kolwicz, S. C., Jr.; Tian, R. *J. Visualized Exp.* **2010**, *42*, 2069.
(28) Wishart, D. S.; Jewison, T.; Guo, A. C.; Wilson, M.; Knox, C.; Liu, Y.; Djoumbou, Y.; Mandal, R.; Aziat, F.; Dong, E.; Bouatra, S.; Sinelnikov, I.; Arndt, D.; Xia, J.; Liu, P.; Yallou, F.; Bjorndahl, T.; Perez-Pineiro, R.; Eisner, R.; Allen, F.; Neveu, V.; Greiner, R.; Scalbert, A. *Nucleic Acids Res.* **2013**, *41*, D801−D807.
(29) Ulrich, E. L.; Akutsu, H.; Doreleijers, J. F.; Harano, Y.; Ioannidis, Y. E.; Lin, J.; Livny, M.; Mading, S.; Maziuk, D.; Miller, Z.; Nakatani, E.; Schulte, C. F.; Tolmie, D. E.; Kent Wenger, R.; Yao, H.; Markley, J. L. *Nucleic Acids Res.* **2007**, *36*, D402−D408.
(30) Agar, N. S.; Rae, C. D.; Chapman, B. E.; Kuchel, P. W. *Comp Biochem Physiol B* **1991**, *99* (3), 575−597.
(31) Karamanlidis, G.; Lee, C. F.; Garcia-Menendez, L.; Kolwicz, S. C., Jr; Suthammarak, W.; Gong, G.; Sedensky, M. M.; Morgan, P. G.; Wang, W.; Tian, R. *Cell Metab.* **2013**, *18* (2), 239−50.
(32) Hsu, C. P.; Oka, S.; Shao, D.; Hariharan, N.; Sadoshima, J. *Circ. Res.* **2009**, *105* (5), 481−91.


DOI: 10.1021/acs.analchem.6b00442
*Anal. Chem.* 2016, 88, 4817−4824